



The Effect of Fracture Stability on the Performance of Locking Plate Fixation in Periprosthetic Femoral Fractures

Mehran Moazen, PhD^{a,b}, Jonathan H. Mak, MEng^a, Lee W. Etchels, MEng^a, Zhongmin Jin, PhD^{a,c}, Ruth K. Wilcox, PhD^a, Alison C. Jones, PhD^a, Eleftherios Tsiridis, MD, PhD, FRCS^{d,e,f}

^a Institute of Medical and Biological Engineering, School of Mechanical Engineering, University of Leeds, Leeds LS2 9JT, UK

^b Medical and Biological Engineering, School of Engineering, University of Hull, Hull HU6 7RX, UK

^c Institute of Advanced Manufacturing Technology, School of Mechanical Engineering, Xi'an Jiaotong University, Xi'an 710049, P.R. of China

^d Academic Department of Orthopaedic and Trauma, University of Leeds, Leeds LS2 9JT, UK

^e Department of Surgery and Cancer, Division of Surgery, Imperial College London, London W12 0HS, UK

^f Academic Orthopaedics and Trauma Unit, Aristotle University Medical School, University Campus 54 124, Thessaloniki, Greece

ARTICLE INFO

Article history:

Received 13 February 2013

Accepted 21 March 2013

Keywords:

fracture movement
weight bearing
strain
stiffness
finite element method

ABSTRACT

Periprosthetic femoral fracture (PFF) fixation failures are still occurring. The effect of fracture stability and loading on PFF fixation has not been investigated and this is crucial for optimum management of PFF. Models of stable and unstable PFFs were developed and used to quantify the effect of fracture stability and loading in a single locking plate fixation. Stress on the plate was higher in the unstable compared to the stable fixation. In the case of unstable fractures, it is possible for a single locking plate fixation to provide the required mechanical environment for callus formation without significant risk of plate fracture, provided partial weight bearing is followed. In cases where partial weight bearing is unlikely, additional biological fixation could be considered.

© 2013 Elsevier Inc. All rights reserved.

Periprosthetic femoral fractures (PFF) can occur following primary total hip arthroplasty (THR) [1–6]. The management of these fractures is becoming increasingly important due to rise in number of THRs [4], but is challenging due to the presence of the underlying prosthesis. Over recent years there have been a number of fixation failures reported in the literature including instances of fixation plate fracture [3,5,7]. Interestingly, it appears that most Vancouver B1 [1] PFF fixation failures were initially transverse fractures [5], considering that if no gap were present at the fracture site postoperatively, these would have been stable fractures with good bone quality. Nevertheless, overloading of the fixation plates can cause local stress concentrations [5] which result in progressive damage over multiple loading cycles and can cause plate fracture. Analysis of the construct geometry and loading conditions which create these peaks of stress is therefore of interest.

Several authors have compared the application of various plates with different configurations of locking and non-locking screws and cables to find the optimum fixation for PFF [8–12]. However, these studies are commonly carried out on a particular fracture configuration and loading with either stainless steel (SS) or titanium (Ti) plate. The success of any one of these fixation constructs also depends on the configuration of the bone fracture and its stability once reduced. For example simple, transverse (stable) fracture may allow for load transfer at the fracture site, where a severely comminuted (unstable) fracture may not.

A number of factors including fracture stability, loading and material properties of the fixation device will play a role in the stiffness of the construct, level of fracture movement and subsequent healing mode of the fracture [13–15]. The effect of fracture stability and loading on either SS or Ti plates in PFF fixation does not appear to have been investigated and this is fundamental for optimum management of PFF.

Experimental *in vitro* models have been commonly used to test different fixation methods for PFF in terms of stiffness, fracture movement or surface strain [8–11]. Computational models based on the finite element (FE) method allow the full pattern of strain and stress distribution to be assessed, as well as providing the flexibility to test a wide range of cases [16–19]. However, the computational model validity needs to be demonstrated [20]. Comparison with

This work is supported by British Orthopaedic Association (BOA) through the Latta Fellowship and was partially funded through WELMEC (Wellcome Trust & EPSRC, under grant WT 088908/Z/09/Z) and LMBRU through NIHR (National Institute for Health Research).

The Conflict of Interest statement associated with this article can be found at <http://dx.doi.org/10.1016/j.arth.2013.03.022>.

Reprint requests: Mehran Moazen, PhD, Medical and Biological Engineering, School of Engineering, University of Hull, Hull HU6 7RX, UK.

experimental in vitro data may be used to provide confidence in the model predictions, but, as yet, such corroborated FE models of PFF fixation are surprisingly rare [18].

In this study a FE model of the fixation of a Vancouver type B1 PFF within a stable stem with good bone quality [1] was developed. The predictions of the model were first compared with experimental tests to corroborate mechanical behaviour, with particular emphasis on the fixation plate. This model was then used to address aims of this study: (1) to quantify the effect of fracture stability on the performance of a locking plate fixation (2) to compare the performance of SS versus Ti plate fixations in stable and unstable fracture under two weight bearing conditions. The overall hypothesis of this study is that fracture stability can considerably affect the performance of both SS and Ti locking plates in PFF fixation.

Materials and Methods

In the first step, FE models of stable (with no gap at the fracture site) and unstable (with a 10 mm gap at the fracture site) periprosthetic fracture cases were developed to match corresponding instrumented experimental models that were mechanically tested in the laboratory. The stiffness, surface strain and fracture movement were compared. Following this, in the second step, the FE models were altered to compare the performance of the SS versus Ti plate in the stable and unstable PFF fixation cases under two weight bearing conditions (Fig. 1).

Experimental Methodology

In a parallel experimental study [21], five PFF fixation models using large left synthetic femurs (fourth generation composite femur, Sawbones Worldwide, WA, USA) were tested and the one with the average stiffness was selected for this study (average specimen). In brief, the femoral condyle (distal 60 mm of the femur) was removed and a total hip arthroplasty was performed using an Exeter femoral stem (V40; size N°0; offset 37.5) and head (28 mm diameter – Stryker, NJ, USA) both made of SS. The stem was inserted into the femoral canal and cemented using polymethylmethacrylate (PMMA) cement (Simplex P, Stryker, NJ, USA). A transverse fracture was created 10 mm below the tip of the stem and completely reduced with an eight hole SS locking plate (length: 155 mm; width: 17.5 mm; thickness: 5 mm) where there was ca. 1 mm of gap at the plate-bone interface. Unicortical screws (outer diameter: 5 mm; length: 13 mm) and bicortical screws (outer diameter: 5 mm; length: 40 mm – Stryker, NJ, USA) were used in the three most proximal and distal holes of the plate respectively, leaving two empty screw holes across the fracture site. The specimen was also taken to Leeds General Infirmary (Leeds, UK) where an antero-posterior x-ray

(Multix Fusion, Siemens, Erlangen, Germany) was taken to evaluate the construct.

The specimen was instrumented with eight uniaxial strain gauges (Tokyo Sokki Kenkyujo, Tokyo, Japan) located on the medial side of the femur 0, 40, 80 and 200 mm below the lesser trochanter (SG1–SG4), on the lateral side of the femur 200 mm below the lesser trochanter (SG5), and on the lateral side of the plate below the third (SG6), fourth (SG7) and fifth (SG8) most proximal screw holes (see Fig. 2). The distal end of the specimen was fully fixed using PMMA cement and grub screws (i.e. non-surgical headless screws used here purely for mechanical purposes) into a cylindrical housing and mounted on a materials testing machine (Instron, MA, USA) at 10° adduction in the frontal plane and aligned vertically in the sagittal plane. This position simulates anatomical one-legged stance [22]. An axial load of 500 N, corresponding to recommended partial weight bearing following stable plate fixation [23] was applied to the femoral head stem via a hemispherical cup.

The stiffness was calculated based on the slope of the load–displacement data obtained from the material testing machine. The strain was measured in all the strain gauges at the maximum load. The fracture movement was recorded using two digital cameras (Canon, Tokyo, Japan) placed on the medial and lateral side of the femur, by photographing before loading and at 500 N. Movements of two markers on each side on the proximal and distal bony fragments were then digitized using a custom written program in MATLAB (MathWorks, MA, USA). Following testing, an unstable fracture was simulated by cutting the bone 5 mm above and below the existing fracture line to increase the fracture gap to 10 mm. The specimen was then reloaded to 500 N and the measurements repeated.

Computational Methodology

Model Development

A computer aided design (CAD) model of the synthetic femur was obtained from Biomed Town through the BEL repository managed by the Intituti Ortopedici Rizzoli (Bologna, Italy) [24]. The model consisted of three segments: the cortical bone and the proximal and distal cancellous bone. CAD files of the stem and locking plate were provided by manufacturer (Stryker, NJ, USA). The model was assembled in SolidWorks (Dassault Systemes, MA, USA). First, virtual total hip arthroplasty was performed where the stem position was determined based on AP and ML radiographs. The cement mantle was reconstructed based on the CT images of a reamed specimen. Second, a transverse fracture was created by dividing the construct into two halves that were fixed using the same screw and plate configuration as the experimental model ('stable model' – Fig. 2). Lastly, a separate model was developed in which a fracture gap of 10 mm was induced similar to the experimental procedure ('unstable model'). In both models, the distal PMMA cement, screws and cylindrical pot that were

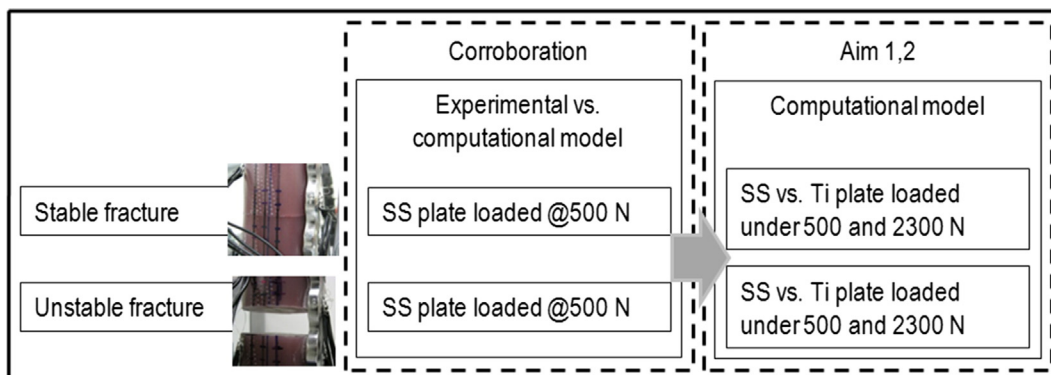


Fig. 1. A schematic of this study.



Fig. 2. Experimental and computational model of PFF fixation. SG1–SG8 highlight the strain gauge attachment area.

used in the experimental model to fix the specimen were also modelled to include the effect of deformation in this region. The models were then exported to a finite element package (ABAQUS v. 6.9, Dassault Systemes, MA, USA) for analysis.

Material Properties

All sections were assigned isotropic material properties with an elastic modulus of 16.3 GPa for cortical bone [25], 0.15 GPa for cancellous bone [18], 2.45 GPa for cement [18], 200 GPa for SS [17] and 110 GPa for Ti [17]. A Poisson's ratio of 0.3 was used for all materials [17].

Interactions

The interfaces at the cancellous to cortical bone, cement to bone, grub screws to cement, and screw head to plate were fixed. Contact conditions were specified with hard normal contact stiffness. A coefficient of friction of 0.3 was used at the stem to cement, housing to cement, plate to bone and bone to bone (i.e. fracture site in the stable model) interfaces [26–29]. Screw-bone interfaces were modeled using an approach described elsewhere [30], which was shown to lead to closer agreement between experimental and computational models when modeling screw-bone fixation. In brief, sliding contact conditions were created at the screw-bone interface, while screw pull-out/push-in was resisted by attaching two spring elements between the screw end and medial side of the bone along the screw shaft. A frictionless contact with normal contact stiffness of 600 N/mm was used [31]. The total spring stiffness of bicortical screws was 3141 N/mm that was halved for the unicortical screws [32], corresponding to reported screw pull-out data.

Boundary Conditions and Loads

The constructs were loaded to replicate the experimental set up. The distal cylindrical pot was fixed in all directions while the stem femoral head was loaded under axial load of 500 N.

Mesh Sensitivity

Tetrahedral (C3D10M) elements were used to mesh all of the components in ABAQUS. Convergence was tested by increasing the number of elements from 70,000 to 1,600,000 in five steps. The solution converged on the parameter of the interest ($\leq 5\%$ – axial stiffness, strain, stress and fracture movement) with over one million elements.

Measurements

In all models, axial stiffness was calculated by dividing the magnitude of axial load by the displacement of the proximal section of the specimen. Strain was averaged from four nodes corresponding to the strain gauge attachment sites in the experimental model. Fracture movement was quantified from the displacement coordinates of the nodes corresponding to the position of the markers in the experiment.

Simulation and Analysis

The outputs of the stable and unstable fracture models were first compared to the experimental results. In the case of the strain measurements, the agreement was measured using the concordance correlation coefficient (CCC) [33]. The properties of the plates and screws in both models were then changed to Ti and the models reanalysed. To test the performance of the PFF fixations under higher loadings that can occur during full weight bearing, all the models were also analysed under axial loading of 2300 N [22].

Results

A comparison between the experimental and computational models in terms of axial stiffness, surface strain measurement and fracture movement showed that:

- (1) The computational models overestimated the axial stiffness of the stable and unstable PFF fixation construct by 121% and 61% respectively. However, computational models predicted 78% reduction in the stiffness of the stable compared to the unstable PFF fixation which is comparable to 70% reduction that was shown by the experimental model (Fig. 3).
- (2) There was a high level of agreement in the strain measurements between the experimental and computational models with a CCC of 0.77 for the stable and 0.8 for unstable construct cases (Fig. 4).
- (3) The computational models underestimated the axial fracture movement. However, both models in the case of stable PFF fixation showed less than 0.1 mm movement whereas in the case of unstable PFF fixation, the movement was in the range of 0.2–0.7 mm. Also both models showed unparallel axial fracture movement between the near and far cortex in both stable and unstable PFF fixation (Fig. 5).

The computational predicted strain values, maximum von Mises stress on the plate, and fracture movement for models with the different plate properties under the two axial loading cases are presented in Tables 1 and 2. The results showed that:

- (1) Strain on the proximal section of the femur (SG1–SG3) was lower in the unstable compared to the stable PFF fixation; nevertheless the strain magnitudes were similar in both cases under the two loading cases and with the two plate materials. The strain in the distal section of the bone was higher in the unstable compared to the stable fixation.

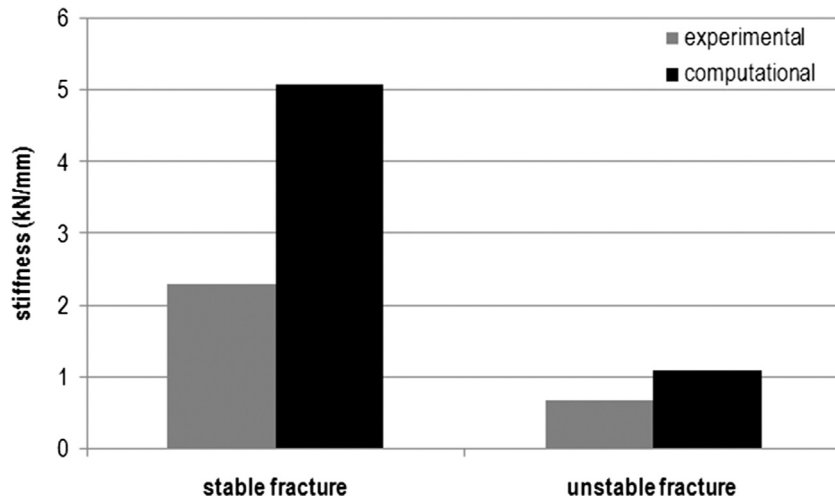


Fig. 3. Comparison between the experimental and computational stiffness of the stable and unstable PFF fixation based on average specimen.

- (2) Strain and stress on the plate were considerably higher in the unstable compared to the stable fixation. For example, the maximum von Mises stress on the SS plate under 500 N loading in unstable PFF fixation was ca. 32 times higher than the stable fixation. Increasing the axial loading from 500 N to 2300 N led to ca. 4.6 times greater maximum von Mises stress on the plate with similar conditions. Further, altering the plate property from SS to Ti led to ca. a 1.3 and 1.1 fold reduction in the maximum von Mises stress on the plate under same loading for stable and unstable PFF fixation respectively.
- (3) Fracture movement in the stable PFF fixation was less than 0.1 mm in all cases, whereas in the unstable fixation at 500 N it was within the range of 0.2–1 mm, and at 2300 N it was above 1 mm for both SS and Ti plate in the medial view. Fracture movement in the medial view was higher than the anterior view.

Maximum von Mises stress in the stable PFF fixation was on the lateral side of the plate across the empty screw hole in all cases, whereas in the unstable fixation it was on the medial side of the plate between the third and fourth screw hole (Fig. 6). In the unstable PFF fixation under 2300 N load, the titanium plate came into contact

across the empty screw hole with the proximal bony fragment this led to a concentration of stress on the plate, however such contact did not occur under same loading condition in the SS plate (Fig. 6).

Discussion

Quantifying the effect of fracture stability and loading on the relative risk of plate fracture for PFF fixations does not appear to have been undertaken previously. In this study an FE model was described and used to quantify the effect of aforementioned parameters in SS and Ti locking plate fixation. In each case, peak stress values were compared with the yield stress and fatigue life (as a result of cyclic loading) for each material, an indication of plate fracture risk.

The FE model was first compared with experimental tests. A strong correlation was found between the strain predictions of the experimental and computational models. However, the computational models overestimated the stiffness of the experimental models. This could be due to a number of factors, such as over-estimation of material or interaction properties. FE models have been shown to be sensitive to the choice of interaction properties at the interfaces [28,30]. The fact that there was a closer agreement between the

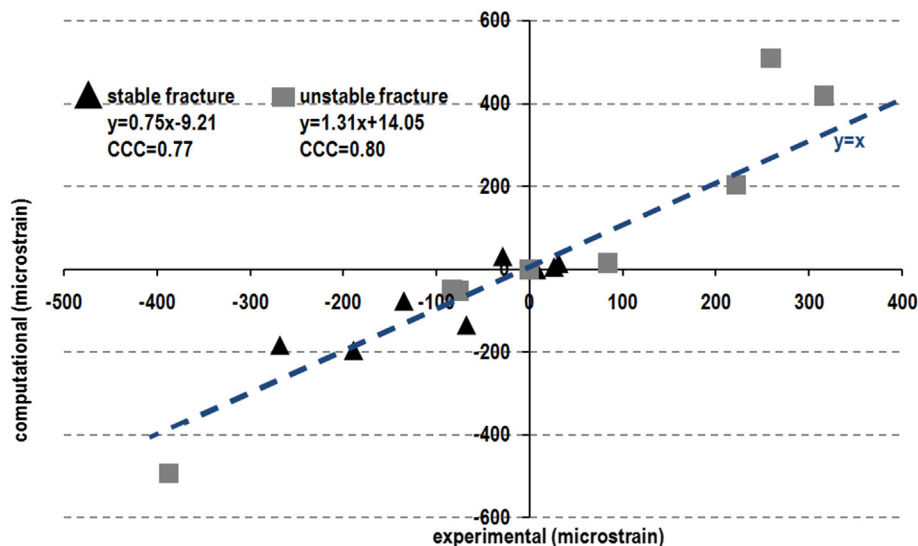


Fig. 4. Comparison between the experimental and computational strain of the stable and unstable PFF fixation based on the average specimen.

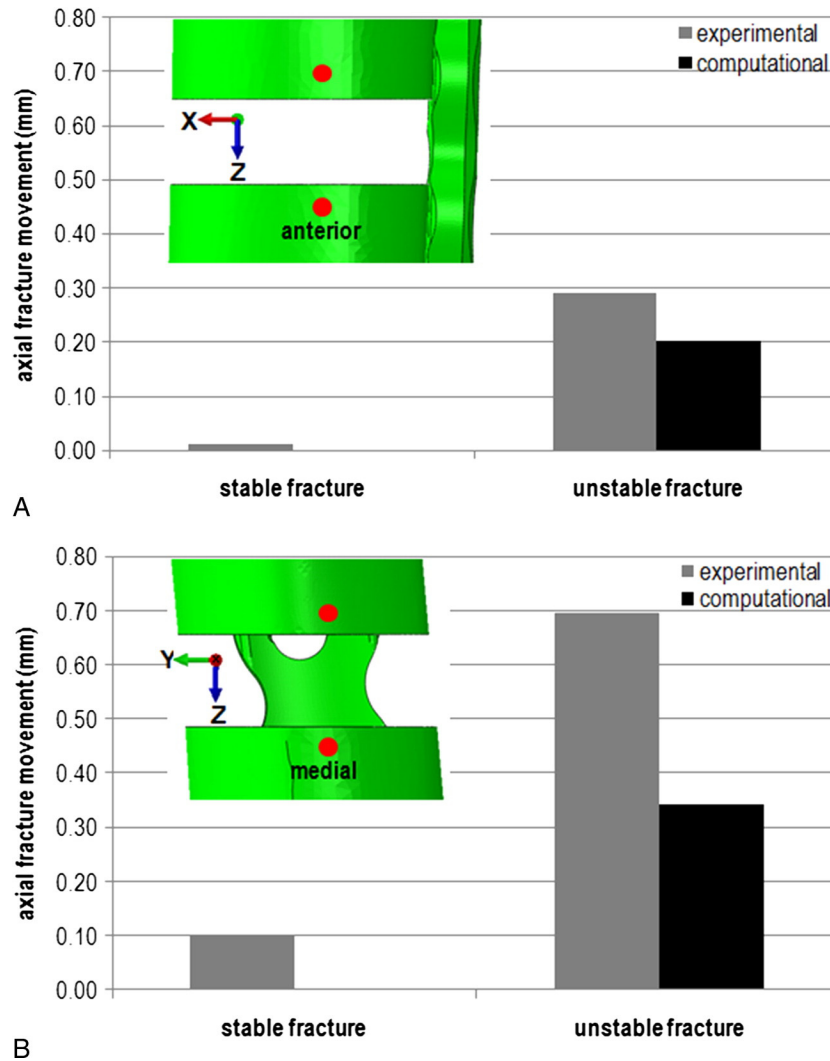


Fig. 5. Comparison between the experimental and computational fracture movement on the anterior (A) and medial (B) view of the stable and unstable PFF fixation based on the average specimen. Note in the stable fracture, the computational axial fracture movements were almost zero.

computational and experimental models of the unstable fracture (i.e. without interaction at fracture site) compared to the stable fracture (i.e. with interactions at fracture site – Fig. 4) indicates that this was one source of error. Despite this overestimation, it was reassuring

that both experimental and computational model captured very similar percentage of reduction in the stiffness of stable compare to unstable PFF fixation (ca. 70% vs. 78% respectively). This, coupled with the good agreement in strain within the area of interest in the fixation plate, provided confidence that the FE model was suitable for making the comparisons between different fixation scenarios required for this study.

Table 1
Summary of the Strain Measurements (SG1-SG8) and Maximum von Mises Stress on the Plate (SVM).

Axial Load (N)	Stable				Unstable			
	500	2300	500	2300	500	2300	500	2300
Material	SS	SS	Ti	Ti	SS	SS	Ti	Ti
SG1	-76	-349	-75	-355	-50	-230	-44	-215
SG2	-196	-916	-197	-918	-52	-260	-44	-263
SG3	-183	-808	-186	-824	-1	-5	-1	-6
SG4	32	157	33	161	419	2059	446	2182
SG5	-134	-624	-135	-628	-493	-2392	-519	-2506
SG6	15	61	20	84	509	2510	816	3813
SG7	6	23	7	28	204	985	274	1447
SG8	0	2	0	0	15	41	-43	-192
SVM (MPa)	8	35	6	28	255	1258	227	1084

Note. Positive values indicate tensile strain and negative values indicate compressive strain.

The overestimation of the stiffness clearly explains the underestimation of the fracture movement predicted by the FE models. Nevertheless, the movement in both experimental and FE models in the stable PFF fixation was below the threshold that is suggested to promote callus formation (0.2-1 mm) [13,14,34]. This rigid fixation explains why callus did not form in some of the previous case reports of rigid PFF fixations [5,19]. Rigid PFF fixation can be avoided by

Table 2
Summary of the Axial Fracture Movement (mm) of PFF Fixation Constructs.

Axial Load (N)	Stable				Unstable			
	500	2300	500	2300	500	2300	500	2300
Material	SS	SS	Ti	Ti	SS	SS	Ti	Ti
Anterior	0.001	0.007	0.001	0.007	0.202	0.973	0.249	1.197
Medial	0.003	0.016	0.003	0.016	0.343	1.665	0.413	1.976

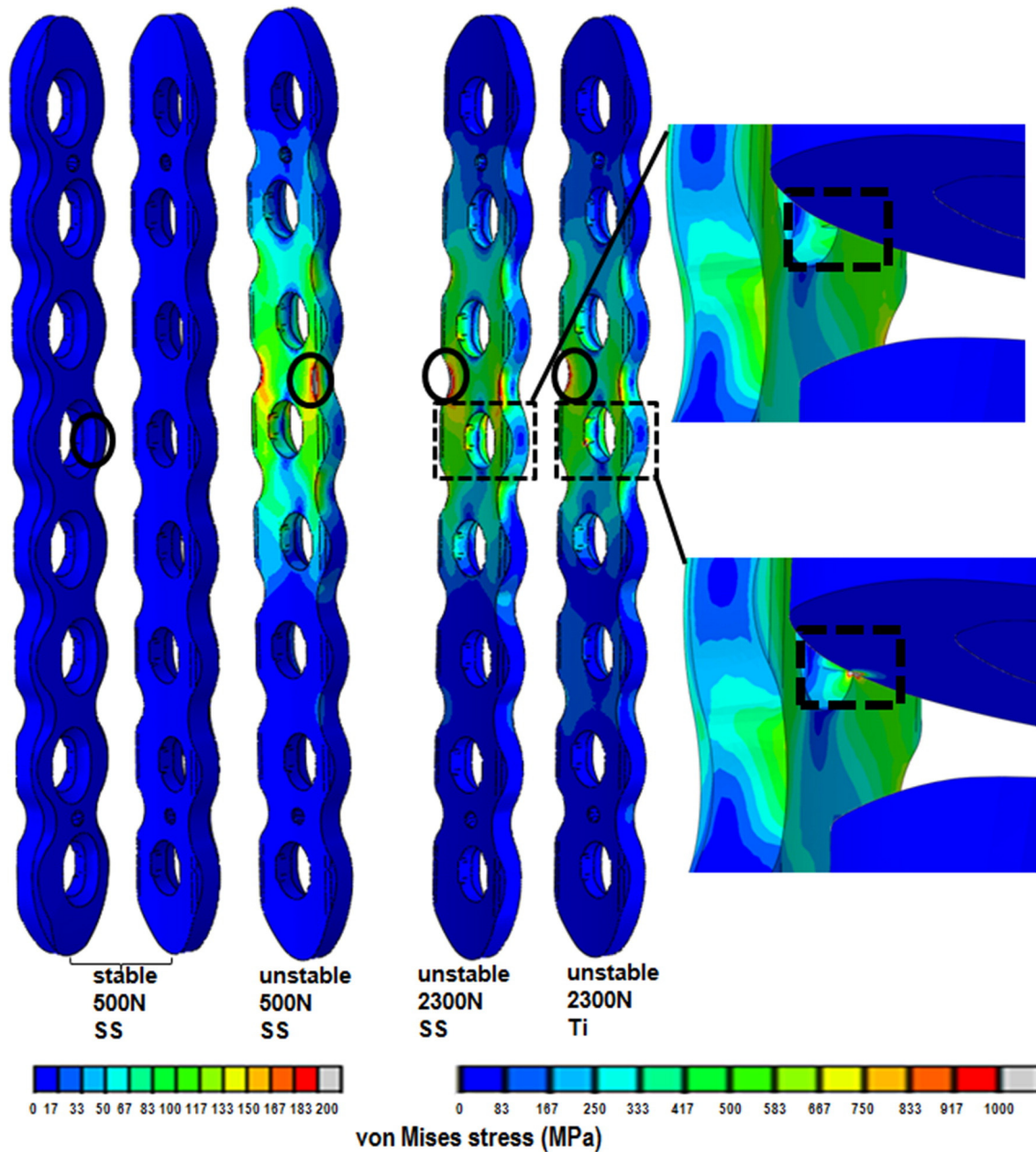


Fig. 6. Comparison between von Mises stress contour plot of all cases. The regions of maximum von Mises stress are highlighted by ovals. Dotted rectangles highlight the plate to bone contact that did not occur in the stainless steel (SS) plate and occurred in the titanium (Ti) plate fixation under high axial loading of 2300 N.

increasing the bridging length [35] or using alternative screw designs such as far cortical locking screws [36].

As anticipated, the load sharing between the plate and the bone in the case of the stable fracture caused higher compressive strain in the proximal bone and reduced tensile strain on the surface of the plate (Table 1), when compared to the unstable fracture cases. Where this load sharing existed, the maximum stress concentrations on the plate did not exceed the fatigue limit (Table 3), even for the equivalent of five years of normal walking [17]. For the unstable fracture cases, where the plate was the sole loading bearing component, maximum plate stress was much higher. In the case of partial weight bearing was within the fatigue limit of the SS and Ti commonly used to manufacture implants (see Table 3). Furthermore, the fracture movement was within the range of 0.2–1 mm [13,14,34]. However, under the higher load of 2300 N, not only was the fracture movement above the aforementioned range but also the von Mises stress reached the yield level of both SS and Ti (Table 3) [17,37], suggesting that

mechanical damage could occur to the plate within a relative small number of cycles.

These findings have two clinical consequences. First, unstable fractures could be potentially treated with a single 5 mm thick SS locking plate using the screw configuration applied in this study provided that patient is restricted to partial weight bearing. Second, in the cases where complete fracture reduction has not been achieved

Table 3
Summary of Yield Stress, Ultimate Tensile Stress and Fatigue Limit of SS and Ti [37].

Material	SS	Ti
ASTM designation	F138, F139	F67
Condition	30% Cold worked	30% Cold worked
Ultimate tensile stress (MPa)	930	760
Yield stress (MPa)	792	485
Fatigue limit (at 107 cycles-MPa)	310–448	300

and a fracture gap is present postoperatively, the patient should be warned that full weight bearing can potentially lead to mechanical failure of the fixation [38]. Nevertheless, orthopedic trauma surgeons may consider long stem revision and bypassing the fracture gap or biological fixation in addition to locking plates in the case of unstable PFF fractures, particularly in active patients [5,8,39].

Results here highlight that fracture stability and postoperative weight bearing can have a more pronounced effect on the performance of plate fixation than the material properties of the fixation, given that other biomechanical factors such as bridging length are the same nevertheless patient variability cannot be ignored [40]. Lujan et al. [41] suggested that Ti plates can enhance callus formation when compared to the SS plate in distal femoral fractures. The present study provides some quantification of the increase in plate bending and fracture movement for Ti, which may contribute to enhanced callus formation. However, the yield stress and fatigue limit of Ti are lower than that of SS (Table 3). Therefore, the risk of failure remains unless early callus formation and the resulting load sharing with the bone can be created through careful postoperative loading.

A noteworthy, unanticipated result occurred in the unstable PFF fixation under axial load of 2300 N, the Ti plate came into contact across the fracture site to the proximal bony fragment (see dotted rectangles in Fig. 6). FE models in this study predicted stress riser effect on the plate fixation as a result of this contact. However, care must be taken in the interpretation of this result since FE models in this study: (1) did not include any failure criteria for the bone or other segments (2) considered a static loading where in reality the fixation construct is under cyclic loading where it is likely that a small bony fragment at the plate–bone contact zone will fail earlier than the plate. Nonetheless, this finding highlights the importance of plate–bone gap particularly in Ti locking plate fixation. Such a gap has been suggested to increase the flexibility of the fixation [42], prevent necrosis and ensure blood supply to the fracture site that plays a crucial role in fracture healing process [43].

In conclusion, in the case of unstable fractures or where a fracture gap is present post operatively, it is possible for a single locking plate fixation to provide the required mechanical environment for callus formation without significant risk of plate fracture, provided partial weight bearing is followed. Full weight bearing significantly increases the risk of plate fracture regardless of the whether SS or Ti plates are used. In cases where partial weight bearing is unlikely, additional biological fixation could be considered. The FE model described in this study will be used in future studies to investigate alternative fixation methods for PFF fixation.

Acknowledgments

We thank Simon M Graham for his assistance during the experimental work. The components for the experimental and computational models were provided by Stryker (SA, Switzerland).

References

- Duncan CP, Masri BA. Fractures of the femur after hip replacement. *Instr Course Lect* 1995;44:293.
- Parvizi J, Rapuri VR, Purtill JJ, et al. Treatment protocol for proximal femoral periprosthetic fractures. *J Bone Joint Surg Am* 2004;86:8.
- Lindahl H, Malchau H, Oden A, et al. Risk factors for failure after treatment of a periprosthetic fracture of the femur. *J Bone Joint Surg Br* 2006;88:26.
- Tsiridis E, Narvani AA, Timperley JA, et al. Dynamic compression plates for Vancouver type B periprosthetic femoral fractures: a 3-year follow-up of 18 cases. *Acta Orthop* 2005;76:531.
- Buttaro MA, Farfalli G, Paredes Nunez M, et al. Locking compression plate fixation of Vancouver type-B1 periprosthetic femoral fractures. *J Bone Joint Surg Am* 2007;89:1964.
- Mont MA, Maar DC. Fractures of the ipsilateral femur after hip arthroplasty. A statistical analysis of outcome based on 487 patients. *J Arthroplasty* 1994;9:511.
- Graham SM, Moazen M, Leonidou A, et al. Locking plate fixation for Vancouver B1 periprosthetic femoral fractures: a critical analysis of 135 cases. *J Orthop Sci* (in press). <http://dx.doi.org/10.1007/s00776-013-0359-4>
- Talbot M, Zdero R, Schemitsch EH. Cyclic loading of periprosthetic fracture fixation constructs. *J Trauma* 2008;64:1308.
- Dennis MG, Simon JA, Kummer FJ, et al. Fixation of periprosthetic femoral shaft fractures occurring at the tip of the stem: a biomechanical study of 5 techniques. *J Arthroplasty* 2000;15:523.
- Peters CL, Bachus KN, Davitt JS. Fixation of periprosthetic femur fractures: a biomechanical analysis comparing cortical strut allograft plates and conventional metal plates. *Orthopedics* 2003;26:695.
- Zdero R, Walker R, Waddell JP, et al. Biomechanical evaluation of periprosthetic femoral fracture fixation. *J Bone Joint Surg Am* 2008;90:1068.
- Moazen M, Jones AC, Jin Z, et al. Periprosthetic fracture fixation of the femur following total hip arthroplasty: a review of biomechanical testing. *Clin Biomech* 2011;26:13.
- Goodship AE, Kenwright J. The influence of induced micromovement upon the healing of experimental tibial fractures. *J Bone Joint Surg Br* 1985;67:250.
- Claes L, Wilke H-J, Augat P, et al. Effect of dynamization of gap healing of diaphyseal fractures under external fixation. *Clin Biomech* 1995;8:227.
- Oh JK, Sahu D, Ahn YH, et al. Effect of fracture gap on stability of compression plate fixation: a finite element study. *J Orthop Res* 2010;28:462.
- Mihalko WM, Beaudoin AJ, Cardea JA, et al. Finite-element modelling of femoral shaft fracture fixation techniques post total hip arthroplasty. *J Biomech* 1992;25:469.
- Chen G, Schmutz B, Wullschlegler M, et al. Computational investigation of mechanical failures of internal plate fixation. *Proc Inst Mech Eng H* 2010;224:119.
- Shah S, Kim SYR, Dubov A, et al. The biomechanics of plate fixation of periprosthetic femoral fractures near the tip of a total hip implant: cables, screws, or both? *Proc Inst Mech Eng H* 2011;225:845.
- Moazen M, Jones AC, Leonidou A, et al. Rigid versus flexible plate fixation for periprosthetic femoral fracture – computer modelling of a clinical case. *Med Eng Phys* 2012;34:1041.
- Anderson AE, Ellis BJ, Weiss JA. Verification, validation, and sensitivity studies in computational biomechanics. *Comput Method Biomech Biomed Eng* 2007;10:171.
- Mak JH, Etchels LW, Moazen M, et al. Locking plates versus long stem fixation to restore pre-fracture mechanics of a B1 periprosthetic femoral fracture. *Proceedings of the 2012 Annual Meeting of Orthopaedic Research Society*. San Francisco, USA.
- Bergmann G, Deuretzbacher G, Heller M, et al. Hip contact forces and gait patterns from routine activities. *J Biomech* 2001;34:859.
- Ryf CR, Arraf J. Postoperative fracture treatment: general considerations. In: Ruedi TP, Buckley RE, Moran CG, editors. *AO principal of fracture management*. 2nd ed. Davos: AO Publishing; 2007. p. 447.
- Desmarais-Trépanier C. femur_sawbone.zip. From the Biomechanics European Laboratory _BEL_, finite element mesh repository. <http://www.tecnio.ior.it/VRLA/>; 2009.
- Heiner AD. Structural properties of fourth-generation composite femurs and tibias. *J Biomech* 2008;41:3282.
- Hayes WC, Perren SM. Plate–bone friction in the compression fixation of fractures. *Clin Orthop* 1972;89:236.
- Shockey JS, Von Fraunhofer JA, Seligson D. A measurement of the coefficient of static friction of human long bones. *Surf Technol* 1985;25:167.
- Mann KA, Bartel DL, Wright TM, et al. Coulomb frictional interfaces in modeling cemented total hip replacements: a more realistic model. *J Biomech* 1995;28:1067.
- Nuno N, Groppetti R, Senin N. Static coefficient of friction between stainless steel and PMMA used in cemented hip and knee implants. *Clin Biomech* 2006;21:956.
- Moazen M, Mak JH, Jones AC, et al. Evaluation of a new approach for modelling the screw–bone interface in a locking plate fixation – a corroboration study. *Proc Inst Mech Eng Part H*. (in press). <http://dx.doi.org/10.1177/0954411913483259>.
- Bernakiewicz M, Viceconti M. The role of parameter identification in finite element contact analysis with reference to orthopaedic biomechanics applications. *J Biomech* 2002;35:61.
- Zdero R, Rose S, Schemitsch EH, et al. Cortical screw pullout strength and effective shear stress in synthetic third generation composite femurs. *J Biomech Eng* 2007;129:289.
- Lin LL. A concordance correlation coefficient to evaluate reproducibility. *Biometrics* 1989;45:255.
- Egol KA, Kubiak EN, Fulkerson E, et al. Biomechanics of locked plates and screws. *J Orthop Trauma* 2004;18:488.
- Stoffel K, Dieter U, Stachowiak G, et al. Biomechanical testing of the LCP- how can stability in locked internal fixators be controlled? *Injury* 2003;34:S-B11.
- Bottlang M, Doornink J, Fitzpatrick DC, et al. Far cortical locking can reduce stiffness of locked plating constructs while retaining construct strength. *J Bone Joint Surg Am* 2009;91:1985.
- Brunski JB. Metals in: classes of materials used in medicine. In: Ratner BD, Hoffman AS, Schoen FJ, et al, editors. *Biomaterials Science: an introduction to material in medicine*. 2nd ed. California: Elsevier Academic Press; 2004. p. 137.
- Augat P, Merk J, Ignatius A, et al. Early, full weight bearing with flexible fixation delays fracture healing. *Clin Orthop Relat Res* 1996;328:194.
- Haddad FS, Duncan CP, Berry DJ, et al. Periprosthetic femoral fractures around well-fixed implants: use of cortical onlay allografts with or without a plate. *J Bone Joint Surg Am* 2002;84:945.
- Henderson CE, Bottlang M, Marsh JL, et al. Does locked plating of periprosthetic supracondylar femur fractures promote bone healing by callus formation? Two cases with opposite outcomes. *Iowa Orthop J* 2008;28:73.
- Lujan TL, Henderson CE, Madey SM, et al. Locked plating of distal femur fracture leads to inconsistent and asymmetric callus formation. *J Orthop Trauma* 2010;24:156.
- Ahmad M, Nanda R, Bajwa AS, et al. Biomechanical testing of the locking compression plate: when does the distance between bone and implant significantly reduce construct stability? *Injury* 2007;38:358.
- Perren SM. Evolution of the internal fixation of long bone fractures. The scientific basis of biological internal fixation: choosing a new balance between stability and biology. *J Bone Joint Surg Br* 2002;84:1093.